Derivation of the three layer model for surface second-harmonic generation

Sean M. Anderson[1] and Bernardo S. Mendoza[1, *]

^{1}Centro de Investigaciones en Óptica, León, Guanajuato, México
(Dated: April 26, 2016)

We develop explicit expressions for the surface second-harmonic radiation yield using the three layer model. We derive expressions that can be applied to systems without and symmetry considerations, and then reduce them for the (111), (110), and (100) surface symmetries.

I. INTRODUCTION

Surface second-harmonic generation (SSHG) has been shown to be an effective, nondestructive and noninvasive probe to study surface and interface properties.[1–8] SSHG spectroscopy is now very cost-effective and popular because it is an efficient method for characterizing the properties of buried interfaces and nanostructures. The high surface sensitivity of SSHG spectroscopy is due to the fact that within the dipole approximation, the bulk second-harmonic generation (SHG) in centrosymmetric materials is identically zero. The SHG process can occur only at the surface where the inversion symmetry is broken.

SSHG is particularly useful for studying the surfaces of centrosymmetric materials. From the theoretical point of view, the calculation of the nonlinear surface susceptibility tensor, $\chi(-2\omega;\omega,\omega)$, proceeds as follows. To mimic the semi-infinite system, one constructs a supercell consisting of a finite slab of material plus a vacuum region. Both the size of the slab and the vacuum region should be such that the value of $\chi(-2\omega;\omega,\omega)$ is well converged. One has to include a cut function to decouple the two halves of the supercell in order to obtain the value of $\chi(-2\omega;\omega,\omega)$ for either half. If the supercell itself is centrosymmetric, the value $\chi(-2\omega;\omega,\omega)$ is identically zero, thus the cut function is of paramount importance.[9,10] The cut function can be generalized to one that is capable of obtaining the value of $\chi(-2\omega;\omega,\omega)$ for any part of the slab. The depth within the slab for which $\chi(-2\omega;\omega,\omega)$ is nonzero can thus be obtained. One can also study how $\chi(-2\omega;\omega,\omega)$ goes to zero towards the middle of the slab where the centrosymmetry of the material is restored.[11] Therefore, for the surface of any centrosymmetric material we can find the thickness of the layer where $\chi(-2\omega;\omega,\omega) \neq 0$.

In this article, based on the above approach for the calculation of $\chi(-2\omega;\omega,\omega)$, we develop a model for the SH radiation from the surface of a centrosymmetric material. We call this model the three layer model, which considers that the SH conversion takes place in a thin layer just below the surface of the material that lies under the vacuum region and above the bulk of the material. Of course, one can replace the vacuum region with any medium as long as it is not SH active. However, most of the experimental setups for measuring the SH radiation take place in vacuum or air. We develop the model and derive general expressions for the SH radiation for the commonly used polarization combinations of the incoming and outgoing electric fields. We particularize the results for the (111), (110), and (100) crystalline surfaces of centrosymmetric materials.

This paper is organized as follows. In Sec. II, we present the relevant equations and theory that describe the SHG yield. In Sec. III, we present the explicit expressions for each combination of input and output polarizations for the (111), (110), and (100) surfaces. Finally, we list our conclusions and final remarks in Sec. IV.

II. THREE LAYER MODEL FOR SSHG RADIATION

In this section we derive the formulas required for the calculation of the SSHG yield, defined by

$$\mathcal{R} = \frac{I(2\omega)}{I^2(\omega)}, \tag{1}$$

with the intensity given by[12]

$$I(\omega) = \begin{cases} \frac{c}{2\pi} n(\omega)|E(\omega)|^2 & \text{(cgs units)} \\[2mm] 2\epsilon_0 c\, n(\omega)|E(\omega)|^2 & \text{(MKS units)} \end{cases}, \tag{2}$$

where $n(\omega) = \sqrt{\epsilon(\omega)}$ is the index of refraction with $\epsilon(\omega)$ the dielectric function, ϵ_0 is the vacuum permittivity, and c the speed of light in vacuum. We use Ref. 13 as a starting point for this work, as the derivation of the three layer

model is direct. In this scheme, we represent the surface by three regions or layers. The first layer is the vacuum region (denoted by v) with a dielectric function $\epsilon_v(\omega) = 1$ from where the fundamental electric field $\mathbf{E}_v(\omega)$ impinges on the material. The second layer is a thin layer (denoted by ℓ) of thickness d characterized by a dielectric function $\epsilon_\ell(\omega)$. It is in this layer where the second harmonic generation takes place. The third layer is the bulk region denoted by b and characterized by $\epsilon_b(\omega)$. Both the vacuum layer and the bulk layer are semi-infinite (see Fig. 1).

To model the electromagnetic response of the three layer model we follow Ref. 13, and assume a polarization sheet of the form

$$\mathbf{P}(\mathbf{r}, t) = \boldsymbol{\mathcal{P}} e^{i\boldsymbol{\kappa} \cdot \mathbf{R}} e^{-i\omega t} \delta(z - z_\beta) + \text{c.c.}, \tag{3}$$

where $\boldsymbol{\mathcal{P}}$ is the nonlinear polarization (given below), $\mathbf{R} = (x, y)$, $\boldsymbol{\kappa}$ is the component of the wave vector $\boldsymbol{\nu}_\beta$ parallel to the surface, and z_β is the position of the sheet within medium β (see Fig. 1). It is shown in Ref. 14 that the solution of the Maxwell equations for the radiated fields $E_{\beta,p\pm}$ and $E_{\beta,s}$, at points $z \neq 0$, with $\mathbf{P}(\mathbf{r}, t)$ acting as a source can be written as

$$(E_{\beta,p\pm}, E_{\beta,s}) = \left(\frac{\gamma i \tilde{\omega}^2}{\tilde{w}_\beta} \hat{\mathbf{p}}_{\beta\pm} \cdot \boldsymbol{\mathcal{P}}, \frac{\gamma i \tilde{\omega}^2}{\tilde{w}_\beta} \hat{\mathbf{s}} \cdot \boldsymbol{\mathcal{P}} \right), \tag{4}$$

where $\gamma = 2\pi$ in cgs units and $\gamma = 1/2\epsilon_0$ in MKS units. $E_{\beta,p\pm}$ represents the electric field for p-polarization propagating downward ($-$) or upward ($+$), and $E_{\beta,s}$ that for s-polarization, both in medium β. Since for s-polarization the field is parallel to the surface there is no need to distinguish the upward or downward direction of propagation as it is needed for the p-polarized fields. Also, $\tilde{\omega} = \omega/c$, and $\hat{\mathbf{s}}$ and $\hat{\mathbf{p}}_{\beta\pm}$ are the unitary vectors for the s and p polarization of the radiated field, respectively. The $\pm$ notation refers to upward ($+$) or downward ($-$) direction of propagation within medium β, as shown in Fig. 1. Thus,

$$\hat{\mathbf{p}}_{\beta\pm}(\omega) = \frac{\kappa(\omega)\hat{\mathbf{z}} \mp \tilde{w}_\beta(\omega)\hat{\boldsymbol{\kappa}}}{\tilde{\omega} n_\beta(\omega)} = \frac{\sin\theta_0 \hat{\mathbf{z}} \mp w_\beta(\omega)\hat{\boldsymbol{\kappa}}}{n_\beta(\omega)}, \tag{5}$$

where $\kappa(\omega) = |\boldsymbol{\kappa}(\omega)| = \tilde{\omega} \sin\theta_0$, $n_\beta(\omega) = \sqrt{\epsilon_\beta(\omega)}$ is the index of refraction of medium β, and z is the direction perpendicular to the surface that points towards the vacuum. Lastly, $\tilde{w}_\beta(\omega) = \tilde{\omega} w_\beta$, where

$$w_\beta(\omega) = \left(\epsilon_\beta(\omega) - \sin^2\theta_0 \right)^{1/2}, \tag{6}$$

with θ_0 the angle of incidence of $\mathbf{E}_v(\omega)$. We choose the plane of incidence along the $\boldsymbol{\kappa}z$ plane, so

$$\hat{\boldsymbol{\kappa}} = \cos\phi \hat{\mathbf{x}} + \sin\phi \hat{\mathbf{y}}, \tag{7}$$

and

$$\hat{\mathbf{s}} = -\sin\phi \hat{\mathbf{x}} + \cos\phi \hat{\mathbf{y}}, \tag{8}$$

where ϕ is the azimuthal angle with respect to the x axis.

In the three layer model, the nonlinear polarization responsible for the SSHG is immersed in the thin $\beta = \ell$ layer, and is given by

$$\mathcal{P}_{\ell,i}(2\omega) = \begin{cases} \chi_{ijk}(-2\omega; \omega, \omega) E_{\ell,j}(\omega) E_{\ell,k}(\omega) & \text{(cgs units)} \\ \epsilon_0 \chi_{ijk}(-2\omega; \omega, \omega) E_{\ell,j}(\omega) E_{\ell,k}(\omega) & \text{(MKS units)} \end{cases}, \tag{9}$$

where the tensor $\boldsymbol{\chi}(-2\omega; \omega, \omega)$ is the surface nonlinear dipolar susceptibility and the Cartesian indices i, j, k are summed over if repeated. We remark that the thickens of the layer ℓ is considered to be much smaller than the wavelength of the fundamental field, thus multiple reflections of both the fundamental and the SH can be neglected. Also, $\chi_{ijk}(-2\omega; \omega, \omega) = \chi_{ikj}(-2\omega; \omega, \omega)$ is the intrinsic permutation symmetry due to the fact that SHG is degenerate in $E_{\ell,j}(\omega)$ and $E_{\ell,k}(\omega)$. For ease of notation, we drop the frequency argument from $\boldsymbol{\chi}(-2\omega; \omega, \omega)$ and we simply write $\boldsymbol{\chi}$ from now on. As it was done in Ref. 13, in presenting the results Eq. (4)-(8) we have taken the polarization sheet (Eq. (3)) to be oscillating at some frequency ω. However, in the following we find it convenient to use ω exclusively to denote the fundamental frequency and $\boldsymbol{\kappa}$ to denote the component of the incident wave vector parallel to the surface. Then the nonlinear generated polarization is oscillating at $\Omega = 2\omega$ and will be characterized by a wave vector parallel to the surface $\mathbf{K} = 2\boldsymbol{\kappa}$. We can carry over Eqs. (3)-(8) simply by replacing the lowercase symbols
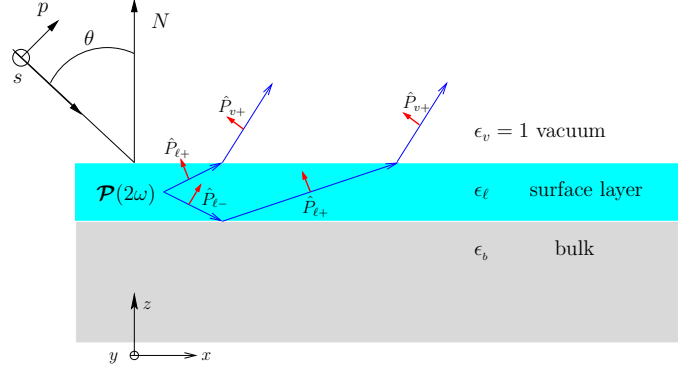
FIG. 1: Sketch of the three layer model for SHG. Vacuum is on top with $\epsilon_v = 1$, the layer with nonlinear polarization $\boldsymbol{\mathcal{P}}(2\omega)$ is characterized with $\epsilon_\ell(\omega)$ and the bulk with $\epsilon_b(\omega)$. In the dipolar approximation the bulk does not radiate SHG. The thin arrows are along the direction of propagation, and the unit vectors for p-polarization are denoted with thick arrows (capital letters denote SH components). The unit vector for s-polarization points along $-y$ (out of the page).

$(\omega, \tilde{\omega}, \boldsymbol{\kappa}, n_\beta, \tilde{w}_\beta, w_\beta, \hat{\mathbf{p}}_{\beta\pm}, \hat{\mathbf{s}})$ with uppercase symbols $(\Omega, \tilde{\Omega}, \mathbf{K}, N_\beta, \tilde{W}_\beta, W_\beta, \hat{\mathbf{P}}_{\beta\pm}, \hat{\mathbf{S}})$, all evaluated at 2ω. We always have that $\hat{\mathbf{S}} = \hat{\mathbf{s}}$.

To describe the propagation of the SH field, we see from Fig. 1, that it is refracted at the layer-vacuum interface (ℓv), and reflected from the layer-bulk (ℓb) and layer-vacuum (ℓv) interfaces, thus we define

$$\mathbf{T}^{\ell v} = \hat{\mathbf{s}} T_s^{\ell v} \hat{\mathbf{s}} + \hat{\mathbf{P}}_{v+} T_p^{\ell v} \hat{\mathbf{P}}_{\ell+}, \tag{10}$$

as the tensor for transmission from the ℓv interface,

$$\mathbf{R}^{\ell b} = \hat{\mathbf{s}} R_s^{\ell b} \hat{\mathbf{s}} + \hat{\mathbf{P}}_{\ell+} R_p^{\ell b} \hat{\mathbf{P}}_{\ell-}, \tag{11}$$

as the tensor of reflection from the ℓb interface, and

$$\mathbf{R}^{\ell v} = \hat{\mathbf{s}} R_s^{\ell v} \hat{\mathbf{s}} + \hat{\mathbf{P}}_{\ell-} R_p^{\ell v} \hat{\mathbf{P}}_{\ell+}, \tag{12}$$

as that from the ℓv interface. The Fresnel factors in uppercase letters, $T_{s,p}^{ij}$ and $R_{s,p}^{ij}$, are evaluated at 2ω from the following well known formulas,[13]

$$t_s^{ij}(\omega) = \frac{2w_i(\omega)}{w_i(\omega) + w_j(\omega)}, \tag{13}$$

$$t_p^{ij}(\omega) = \frac{2w_i(\omega)\sqrt{\epsilon_i(\omega)\epsilon_j(\omega)}}{w_i(\omega)\epsilon_j(\omega) + w_j(\omega)\epsilon_i(\omega)}, \tag{14}$$

$$r_s^{ij}(\omega) = \frac{w_i(\omega) - w_j(\omega)}{w_i(\omega) + w_j(\omega)}, \tag{15}$$

$$r_p^{ij}(\omega) = \frac{w_i(\omega)\epsilon_j(\omega) - w_j\epsilon_i(\omega)}{w_i(\omega)\epsilon_j(\omega) + w_j(\omega)\epsilon_i(\omega)}. \tag{16}$$

From these expressions one can show that,

$$\begin{aligned} 1 + r_s^{\ell b} &= t_s^{\ell b} \\ 1 + r_p^{\ell b} &= \frac{n_b}{n_\ell} t_p^{\ell b} \\ 1 - r_p^{\ell b} &= \frac{n_\ell}{n_b} \frac{w_b}{w_\ell} t_p^{\ell b} \\ t_{s,p}^{\ell v} &= \frac{w_\ell}{w_v} t_{s,p}^{v\ell}. \end{aligned} \tag{17}$$

A. SSHG Yield

As explained above, we neglect multiple reflections, and then we obtain the total 2ω radiated field by using Eqs. (10), (11), and (12),

$$\mathbf{E}(2\omega) = E_s(2\omega)\left(\mathbf{T}^{\ell v} + \mathbf{T}^{\ell v} \cdot \mathbf{R}^{\ell b}\right)\cdot \hat{\mathbf{s}} + E_{p+}(2\omega)\mathbf{T}^{\ell v} \cdot \hat{\mathbf{P}}_{\ell+} + E_{p-}(2\omega)\mathbf{T}^{\ell v}\cdot\mathbf{R}^{\ell b}\cdot\hat{\mathbf{P}}_{\ell-}.$$

The first term is the transmitted s-polarized field, the second one is the reflected and then transmitted s-polarized field and the third and fourth terms are the equivalent fields for p-polarization. The transmission is from the layer into vacuum, and the reflection between the layer and the bulk. After some simple algebra, we obtain

$$\mathbf{E}_\ell(2\omega) = \frac{\gamma i\tilde{\Omega}}{W_\ell}\mathbf{H}_\ell \cdot \boldsymbol{\mathcal{P}}_\ell(2\omega), \tag{18}$$

where,

$$\mathbf{H}_\ell = \hat{\mathbf{s}}\,T_s^{\ell v}\left(1 + R_s^{\ell b}\right)\hat{\mathbf{s}} + \hat{\mathbf{P}}_{v+}T_p^{\ell v}\left(\hat{\mathbf{P}}_{\ell+} + R_p^{\ell b}\hat{\mathbf{P}}_{\ell-}\right). \tag{19}$$

The magnitude of the radiated SH field is given by $E(2\omega) = \hat{\mathbf{e}}^{\mathrm{F}} \cdot \mathbf{E}_\ell(2\omega)$, where $\hat{\mathbf{e}}^{\mathrm{F}}$ is the unit vector of the final polarization, with $\mathrm{F} = S, P$, and then, $\hat{\mathbf{e}}^S = \hat{\mathbf{s}}$ and $\hat{\mathbf{e}}^P = \hat{\mathbf{P}}_{v+}$. We expand the second term in parenthesis of Eq. (19) as

$$\hat{\mathbf{P}}_{\ell+} + R_p^{\ell b}\hat{\mathbf{P}}_{\ell-} = \frac{\sin\theta_0\hat{\mathbf{z}} - W_\ell\hat{\boldsymbol{\kappa}}}{N_\ell} + R_p^{\ell b}\frac{\sin\theta_0\hat{\mathbf{z}} + W_\ell\hat{\boldsymbol{\kappa}}}{N_\ell}$$

$$= \frac{1}{N_\ell}\left(\sin\theta_0(1 + R_p^{\ell b})\hat{\mathbf{z}} - W_\ell(1 - R_p^{\ell b})\hat{\boldsymbol{\kappa}}\right)$$

$$= \frac{T_p^{\ell b}}{N_\ell^2 N_b}\left(N_b^2\sin\theta_0\hat{\mathbf{z}} - N_\ell^2 W_b\hat{\boldsymbol{\kappa}}\right),$$

and rewrite Eq. (18) as

$$E(2\omega) = \frac{2\gamma i\omega}{cW_\ell}\hat{\mathbf{e}}^{\mathrm{F}} \cdot \mathbf{H}_\ell \cdot \boldsymbol{\mathcal{P}}_\ell(2\omega) = \frac{2\gamma i\omega}{cW_v}\mathbf{e}_\ell^{2\omega,\mathrm{F}} \cdot \boldsymbol{\mathcal{P}}_\ell(2\omega), \tag{20}$$

where

$$\mathbf{e}_\ell^{2\omega,\mathrm{F}} = \hat{\mathbf{e}}^{\mathrm{F}} \cdot \left[\hat{\mathbf{s}}T_s^{v\ell}T_s^{\ell b}\hat{\mathbf{s}} + \hat{\mathbf{P}}_{v+}\frac{T_p^{v\ell}T_p^{\ell b}}{N_\ell^2 N_b}\left(N_b^2\sin\theta_0\hat{\mathbf{z}} - N_\ell^2 W_b\hat{\boldsymbol{\kappa}}\right)\right]. \tag{21}$$

In the three layer model the nonlinear polarization is located in layer ℓ, thus, we evaluate the fundamental field required in Eq. (9) in this layer as well. We write

$$\mathbf{E}_\ell(\omega) = E_0\left(\hat{\mathbf{s}}t_s^{v\ell}(1 + r_s^{\ell b})\hat{\mathbf{s}} + \hat{\mathbf{p}}_{\ell-}t_p^{v\ell}\hat{\mathbf{p}}_{v-} + \hat{\mathbf{p}}_{\ell+}t_p^{v\ell}r_p^{\ell b}\hat{\mathbf{p}}_{v-}\right)\cdot\hat{\mathbf{e}}^{\mathrm{in}} = E_0\mathbf{e}_\ell^\omega, \tag{22}$$

and following the steps that lead to Eq. (21), we find that

$$\mathbf{e}_\ell^{\omega,\mathrm{i}} = \left[\hat{\mathbf{s}}t_s^{v\ell}t_s^{\ell b}\hat{\mathbf{s}} + \frac{t_p^{v\ell}t_p^{\ell b}}{n_\ell^2 n_b}\left(n_b^2\sin\theta_0\hat{\mathbf{z}} + n_\ell^2 w_b\hat{\boldsymbol{\kappa}}\right)\hat{\mathbf{p}}_{v-}\right]\cdot\hat{\mathbf{e}}^{\mathrm{i}}. \tag{23}$$

Replacing $\mathbf{E}(\omega) \to E_0\mathbf{e}_\ell^{\omega,\mathrm{i}}$, in Eq. (9), we obtain that

$$\boldsymbol{\mathcal{P}}_\ell(2\omega) = \begin{cases} E_0^2\,\boldsymbol{\chi} : \mathbf{e}_\ell^{\omega,\mathrm{i}}\mathbf{e}_\ell^{\omega,\mathrm{i}} & \text{(cgs units)} \\[2mm] \epsilon_0 E_0^2\,\boldsymbol{\chi} : \mathbf{e}_\ell^{\omega,\mathrm{i}}\mathbf{e}_\ell^{\omega,\mathrm{i}} & \text{(MKS units)} \end{cases}, \tag{24}$$

where $\mathbf{e}_\ell^{\omega,\mathrm{i}}$ is given by Eq. (23), and thus Eq. (20) reduces to ($W_v = \cos\theta_0$)

$$E(2\omega) = \frac{2\eta i\omega}{c\cos\theta_0}\mathbf{e}_\ell^{2\omega,\mathrm{F}} \cdot \boldsymbol{\chi} : \mathbf{e}_\ell^{\omega,\mathrm{i}}\mathbf{e}_\ell^{\omega,\mathrm{i}}, \tag{25}$$

where $\eta = 2\pi$ for cgs units and $\eta = 1/2$ for MKS units. For ease of notation, we define

$$\Upsilon_{\mathrm{iF}} \equiv \mathbf{e}_\ell^{2\omega,\mathrm{F}} \cdot \boldsymbol{\chi} : \mathbf{e}_\ell^{\omega,\mathrm{i}} \mathbf{e}_\ell^{\omega,\mathrm{i}}. \tag{26}$$

From Eqs. (1), (2), and (25) we obtain that

$$\mathcal{R}_{\mathrm{iF}} = \frac{\eta \omega^2}{c^3 \cos^2 \theta_0} \left| \frac{1}{n_\ell} \Upsilon_{\mathrm{iF}} \right|^2, \tag{27}$$

as the SSHG yield, where $\eta = 32\pi^3$ for cgs units and $\eta = 1/(2\epsilon_0)$ in MKS units. Since $\boldsymbol{\chi}$ is a surface second order nonlinear susceptibility, in the MKS unit system is given in m^2/V, and thus $\mathcal{R}_{\mathrm{iF}}$ is given in m^2/W.

III. $\mathcal{R}_{\mathrm{iF}}$ FOR DIFFERENT POLARIZATION CASES

We obtain $\mathcal{R}_{\mathrm{iF}}$ from Eq. (27) for the most commonly used polarizations of incoming and outgoing fields, i.e., iF=pP, pS, sP or sS. For this, we have to explicitly expand Υ_{iF} (Eq. (26)). First, by substituting Eqs. (7) and (8) into Eq. (21), we obtain

$$\mathbf{e}_\ell^{2\omega,\mathrm{P}} = \frac{T_p^{v\ell} T_p^{\ell b}}{N_\ell^2 N_b} \left(N_b^2 \sin \theta_0 \hat{\mathbf{z}} - N_\ell^2 W_b \cos \phi \hat{\mathbf{x}} - N_\ell^2 W_b \sin \phi \hat{\mathbf{y}} \right), \tag{28}$$

for P ($\hat{\mathbf{e}}^{\mathrm{F}} = \hat{\mathbf{P}}_{v+}$) outgoing polarization, and

$$\mathbf{e}_\ell^{2\omega,\mathrm{S}} = T_s^{v\ell} T_s^{\ell b} \left[-\sin \phi \hat{\mathbf{x}} + \cos \phi \hat{\mathbf{y}} \right]. \tag{29}$$

for S ($\hat{\mathbf{e}}^{\mathrm{F}} = \hat{\mathbf{s}}$) outgoing polarization. Secondly, using again Eqs. (7) and (8), but now with Eq. (23), we obtain for p incoming polarization ($\hat{\mathbf{e}}^{\mathrm{i}} = \hat{\mathbf{p}}_{v-}$),

$$\mathbf{e}_\ell^{\omega,\mathrm{P}} \mathbf{e}_\ell^{\omega,\mathrm{P}} = \left(\frac{t_p^{v\ell} t_p^{\ell b}}{n_\ell^2 n_b} \right)^2 \left(n_\ell^4 w_b^2 \cos^2 \phi \hat{\mathbf{x}} \hat{\mathbf{x}} + 2 n_\ell^4 w_b^2 \sin \phi \cos \phi \hat{\mathbf{x}} \hat{\mathbf{y}} + 2 n_\ell^2 n_b^2 w_b \sin \theta_0 \cos \phi \hat{\mathbf{x}} \hat{\mathbf{z}} \right.$$
$$\left. + n_\ell^4 w_b^2 \sin^2 \phi \hat{\mathbf{y}} \hat{\mathbf{y}} + 2 n_\ell^2 n_b^2 w_b \sin \theta_0 \sin \phi \hat{\mathbf{y}} \hat{\mathbf{z}} + n_b^4 \sin^2 \theta_0 \hat{\mathbf{z}} \hat{\mathbf{z}} \right), \tag{30}$$

and for s incoming polarization ($\hat{\mathbf{e}}^{\mathrm{i}} = \hat{\mathbf{s}}$),

$$\mathbf{e}_\ell^{\omega,\mathrm{s}} \mathbf{e}_\ell^{\omega,\mathrm{s}} = \left(t_s^{v\ell} t_s^{\ell b} \right)^2 \left(\sin^2 \phi \hat{\mathbf{x}} \hat{\mathbf{x}} + \cos^2 \phi \hat{\mathbf{y}} \hat{\mathbf{y}} - 2 \sin \phi \cos \phi \hat{\mathbf{x}} \hat{\mathbf{y}} \right). \tag{31}$$

So to calculate $\mathcal{R}_{\mathrm{iF}}$, we summarize in Table I the combination of the equations needed for all four polarization cases. In the following subsections we write down the explicit expressions for Υ_{iF} for the most general case where the surface has no symmetry other than that of noncentrosymmetry. We then develop these expressions for particular cases of the most commonly investigated surfaces, the (111), (100), and (110) crystallographic faces. For ease of writing we split Υ_{iF} as

$$\Upsilon_{\mathrm{iF}} = \Gamma_{\mathrm{iF}} \, r_{\mathrm{iF}}, \tag{32}$$

and in Table II we list, for each surface, the components of $\boldsymbol{\chi}$ different from zero.[15,16]

Case	$\hat{\mathbf{e}}^{\mathrm{F}}$	$\hat{\mathbf{e}}^{\mathrm{i}}$	$\mathbf{e}_\ell^{2\omega,\mathrm{F}}$	$\mathbf{e}_\ell^{\omega,\mathrm{i}} \mathbf{e}_\ell^{\omega,\mathrm{i}}$
$\mathcal{R}_{pP}$	$\hat{\mathbf{P}}_{v+}$	$\hat{\mathbf{p}}_{v-}$	Eq. (28)	Eq. (30)
$\mathcal{R}_{pS}$	$\hat{\mathbf{S}}$	$\hat{\mathbf{p}}_{v-}$	Eq. (29)	Eq. (30)
$\mathcal{R}_{sP}$	$\hat{\mathbf{P}}_{v+}$	$\hat{\mathbf{s}}$	Eq. (28)	Eq. (31)
$\mathcal{R}_{sS}$	$\hat{\mathbf{S}}$	$\hat{\mathbf{s}}$	Eq. (29)	Eq. (31)

TABLE I: Polarization unit vectors for $\hat{\mathbf{e}}^{\mathrm{F}}$ and $\hat{\mathbf{e}}^{\mathrm{i}}$, and equations describing $\mathbf{e}_\ell^{2\omega,\mathrm{F}}$ and $\mathbf{e}_\ell^{\omega,\mathrm{i}} \mathbf{e}_\ell^{\omega,\mathrm{i}}$ for each polarization case.

(111)-C_{3v}	(110)-C_{2v}	(100)-C_{4v}
χ_{zzz}	χ_{zzz}	χ_{zzz}
$\chi_{zxx} = \chi_{zyy}$	$\chi_{zxx} \neq \chi_{zyy}$	$\chi_{zxx} = \chi_{zyy}$
$\chi_{xxz} = \chi_{yyz}$	$\chi_{xxz} \neq \chi_{yyz}$	$\chi_{xxz} = \chi_{yyz}$
$\chi_{xxx} = -\chi_{xyy} = -\chi_{yyx}$		

TABLE II: Components of $\boldsymbol{\chi}$ for the (111), (110) and (100) crystallographic faces, belonging to the C_{3v}, C_{2v}, and C_{4v}, symmetry groups, respectively. For the (111) surface we choose the x and y axes along the $[11\bar{2}]$ and $[1\bar{1}0]$ directions, respectively. For the (110) and (100) we consider the y axis perpendicular to the plane of symmetry.[15] We remark that in general $\boldsymbol{\chi}^{(111)} \neq \boldsymbol{\chi}^{(110)} \neq \boldsymbol{\chi}^{(100)}$.

A. $\mathcal{R}_{pP}$

Per Table I, $\mathcal{R}_{pP}$ requires Eqs. (28) and (30). After some algebra, we obtain that

$$\Gamma_{pP} = \frac{T_p^{v\ell} T_p^{\ell b}}{N_\ell^2 N_b} \left(\frac{t_p^{v\ell} t_p^{\ell b}}{n_\ell^2 n_b} \right)^2. \tag{33}$$

and

$$
\begin{aligned}
r_{pP} = &-N_\ell^2 W_b \big(+ n_\ell^4 w_b^2 \cos^3 \phi \chi_{xxx} + 2 n_\ell^4 w_b^2 \sin \phi \cos^2 \phi \chi_{xxy} + 2 n_b^2 n_\ell^2 w_b \sin \theta_0 \cos^2 \phi \chi_{xxz} \\
&\quad + n_\ell^4 w_b^2 \sin^2 \phi \cos \phi \chi_{xyy} + 2 n_b^2 n_\ell^2 w_b \sin \theta_0 \sin \phi \cos \phi \chi_{xyz} + n_b^4 \sin^2 \theta_0 \cos \phi \chi_{xzz} \big) \\
&-N_\ell^2 W_b \big(+ n_\ell^4 w_b^2 \sin \phi \cos^2 \phi \chi_{yxx} + 2 n_\ell^4 w_b^2 \sin^2 \phi \cos \phi \chi_{yxy} + 2 n_b^2 n_\ell^2 w_b \sin \theta_0 \sin \phi \cos \phi \chi_{yxz} \\
&\quad + n_\ell^4 w_b^2 \sin^3 \phi \chi_{yyy} + 2 n_b^2 n_\ell^2 w_b \sin \theta_0 \sin^2 \phi \chi_{yyz} + n_b^4 \sin^2 \theta_0 \sin \phi \chi_{yzz} \big) \\
&+N_b^2 \sin \theta_0 \big(+ n_\ell^4 w_b^2 \cos^2 \phi \chi_{zxx} + 2 n_\ell^4 w_b^2 \sin \phi \cos \phi \chi_{zxy} + n_\ell^4 w_b^2 \sin^2 \phi \chi_{zyy} \\
&\quad + 2 n_\ell^2 n_b^2 w_b \sin \theta_0 \cos \phi \chi_{zzx} + 2 n_\ell^2 n_b^2 w_b \sin \theta_0 \sin \phi \chi_{zzy} + n_b^4 \sin^2 \theta_0 \chi_{zzz} \big),
\end{aligned} \tag{34}
$$

where all 18 independent components of $\boldsymbol{\chi}$ valid for a surface with no symmetries contribute to $\mathcal{R}_{pP}$. Recall that $\chi_{ijk} = \chi_{ikj}$. Using Table II, we present the expressions for each of the three surfaces being considered here. For the (111) surface we obtain

$$r_{pP}^{(111)} = N_b^2 \sin \theta_0 (n_b^4 \sin^2 \theta_0 \chi_{zzz} + n_\ell^4 w_b^2 \chi_{zxx}) - n_\ell^2 N_\ell^2 w_b W_b (2 n_b^2 \sin \theta_0 \chi_{xxz} + n_\ell^2 w_b \chi_{xxx} \cos 3\phi). \tag{35}$$

where the three-fold azimuthal symmetry of the SHG signal, typical of the C_{3v} symmetry group, is seen in the 3ϕ argument of the cosine function. For the (110) we have that

$$
\begin{aligned}
r_{pP}^{(110)} = &N_b^2 \sin \theta_0 \left[n_b^4 \sin^2 \theta_0 \chi_{zzz} + n_\ell^4 w_b^2 \left(\frac{\chi_{zyy} + \chi_{zxx}}{2} + \frac{\chi_{zyy} - \chi_{zxx}}{2} \cos 2\phi \right) \right] \\
&- 2 n_b^2 n_\ell^2 N_\ell^2 w_b W_b \sin \theta_0 \left(\frac{\chi_{yyz} + \chi_{xxz}}{2} + \frac{\chi_{yyz} - \chi_{xxz}}{2} \cos 2\phi \right).
\end{aligned} \tag{36}
$$

The two-fold azimuthal symmetry of the SHG signal, typical of the C_{2v} symmetry group, is seen in the 2ϕ argument of the cosine function. For the (100) surface we simply make $\chi_{zxx} = \chi_{zyy}$ and $\chi_{xxz} = \chi_{yyz}$, as seen from Table II, and above expression reduces to

$$r_{pP}^{(100)} = N_b^2 \sin \theta_0 \left(n_b^4 \sin^2 \theta_0 \chi_{zzz} + n_\ell^4 w_b^2 \chi_{zxx} \right) - 2 n_b^2 n_\ell^2 N_\ell^2 w_b W_b \sin \theta_0 \chi_{xxz}. \tag{37}$$

where we mention that the azimutal 4ϕ symmetry for the C_{4v} group of the (100) surface is absent in above expresion since such contribution is only related to the bulk nonlinear quadrupolar SH term,[15] that is neglected in this work.

B. $\mathcal{R}_{pS}$

Per Table I, $\mathcal{R}_{pS}$ requires Eqs. (29) and (30). After some algebra, we obtain that

$$\Gamma_{pS} = T_s^{v\ell} T_s^{\ell b} \left(\frac{t_p^{v\ell} t_p^{\ell b}}{n_\ell^2 n_b} \right)^2. \tag{38}$$

and

$$
\begin{aligned}
r_{pS} = &- n_\ell^4 w_b^2 \sin\phi \cos^2\phi \chi_{xxx} - 2n_\ell^4 w_b^2 \sin^2\phi \cos\phi \chi_{xxy} - 2n_\ell^2 n_b^2 w_b \sin\theta_0 \sin\phi \cos\phi \chi_{xxz} \\
&- n_\ell^4 w_b^2 \sin^3\phi \chi_{xyy} - 2n_\ell^2 n_b^2 w_b \sin\theta_0 \sin^2\phi \chi_{xyz} - n_b^4 \sin^2\theta_0 \sin\phi \chi_{xzz} \\
&+ n_\ell^4 w_b^2 \cos^3\phi \chi_{yxx} + 2n_\ell^4 w_b^2 \sin\phi \cos^2\phi \chi_{yxy} + 2n_\ell^2 n_b^2 w_b \sin\theta_0 \cos^2\phi \chi_{yxz} \\
&+ n_\ell^4 w_b^2 \sin^2\phi \cos\phi \chi_{yyy} + 2n_\ell^2 n_b^2 w_b \sin\theta_0 \sin\phi \cos\phi \chi_{yyz} + n_b^4 \sin^2\theta_0 \cos\phi \chi_{yzz},
\end{aligned}
\tag{39}
$$

In this case 12 out of the 18 components of χ valid for a surface with no symmetries, contribute to $\mathcal{R}_{pS}$. This is so, because there is no $\mathcal{P}_{\ell,z}$ component, as the outgoing polarization is S. From Table II we obtain,

$$
r_{pS}^{(111)} = -n_\ell^4 w_b^2 \chi_{xxx} \sin 3\phi,
\tag{40}
$$

for the (111) surface,

$$
r_{pS}^{(110)} = n_\ell^2 n_b^2 w_b \sin\theta_0 (\chi_{yyz} - \chi_{xxz}) \sin 2\phi,
\tag{41}
$$

for the (110) surface, finally,

$$
r_{pS}^{(100)} = 0,
\tag{42}
$$

for the (100) surface, where again, the zero value is only surface related as we neglect the bulk nonlinear quadrupolar contribution.

C. $\mathcal{R}_{sP}$

Per Table I, $\mathcal{R}_{sP}$ requires Eqs. (28) and (31). After some algebra, we obtain that

$$
\Gamma_{sP} = \frac{T_p^{v\ell} T_p^{\ell b}}{N_\ell^2 N_b} \left(t_s^{v\ell} t_s^{\ell b} \right)^2.
\tag{43}
$$

and

$$
\begin{aligned}
r_{sP} = &N_\ell^2 W_b \left(-\sin^2\phi \cos\phi \chi_{xxx} + 2\sin\phi \cos^2\phi \chi_{xxy} - \cos^3\phi \chi_{xyy} \right) \\
&+ N_\ell^2 W_b \left(-\sin^3\phi \chi_{yxx} + 2\sin^2\phi \cos\phi \chi_{yxy} - \sin\phi \cos^2\phi \chi_{yyy} \right) \\
&+ N_b^2 \sin\theta_0 \left(+\sin^2\phi \chi_{zxx} - 2\sin\phi \cos\phi \chi_{zxy} + \cos^2\phi \chi_{zyy} \right),
\end{aligned}
\tag{44}
$$

In this case 9 out of the 18 components of $\chi(2\omega)$ valid for a surface with no symmetries, contribute to $\mathcal{R}_{sP}$. This is so, because there is no $E_z(\omega)$ component, as the incoming polarization is s. From Table II we get,

$$
r_{sP}^{(111)} = N_b^2 \sin\theta_0 \chi_{zxx} + N_\ell^2 W_b \chi_{xxx} \cos 3\phi.
\tag{45}
$$

for the (111) surface,

$$
r_{sP}^{(110)} = N_b^2 \sin\theta_0 \left(\frac{\chi_{zxx} + \chi_{zyy}}{2} + \frac{\chi_{zyy} - \chi_{zxx}}{2} \cos 2\phi \right).
\tag{46}
$$

for the (110) surface, and

$$
r_{sP}^{(100)} = N_b^2 \sin\theta_0 \chi_{zxx}.
\tag{47}
$$

for the (100) surface.

D. $\mathcal{R}_{sS}$

Per Table I, $\mathcal{R}_{sS}$ requires Eqs. (29) and (31). After some algebra, we obtain that

$$\Gamma_{sS} = T_s^{v\ell} T_s^{\ell b} \left(t_s^{v\ell} t_s^{\ell b} \right)^2. \tag{48}$$

and

$$r_{sS} = -\sin^3 \phi \chi_{xxx} + 2\sin^2 \phi \cos \phi \chi_{xxy} - \sin \phi \cos^2 \phi \chi_{xyy} + \sin^2 \phi \cos \phi \chi_{yxx} - 2\sin \phi \cos^2 \phi \chi_{yxy} + \cos^3 \phi \chi_{yyy}. \tag{49}$$

In this case 6 out of the 18 components of $\boldsymbol{\chi}(2\omega)$ valid for a surface with no symmetries, contribute to $\mathcal{R}_{sS}$. This is so, because there is neither an $E_z(\omega)$ component, as the incoming polarization is s, nor a $\mathcal{P}_{\ell,z}(2\omega)$ component, as the outgoing polarization is S. From Table II, we get

$$r_{sS}^{(111)} = \chi_{xxx} \sin 3\phi, \tag{50}$$

for the (111) surface,

$$r_{sS}^{(110)} = 0, \tag{51}$$

and

$$r_{sS}^{(100)} = 0, \tag{52}$$

for the (110) and (100) surfaces, respectively, both being zero as the bulk nonlinear quadrupolar contribution is not considered here.

IV. CONCLUSIONS

We have derived the complete expressions for the SSHG radiation using the three layer model to describe the radiating system. Our derivation yields the full expressions for the radiation that include all required components of χ_{ijk}, regardless of symmetry considerations. Thus, these expressions can be applied to any surface symmetry. We also reduce them according to the most commonly used surface symmetries, the (111), (110), and (100) cases.

---

* Electronic address: bms@cio.mx

[1] C. K. Chen, A. R. B. de Castro, and Y. R. Shen. Surface-enhanced second-harmonic generation. *Phys. Rev. Lett.*, 46(2):145–148, January 1981. I

[2] Y. R. Shen. Surface properties probed by second-harmonic and sum-frequency generation. *Nature*, 337(6207):519–525, February 1989.

[3] J. F. McGilp, M. Cavanagh, J. R. Power, and J. D. O'Mahony. Probing semiconductor interfaces using nonlinear optical spectroscopy. *Opt. Eng.*, 33(12):3895–3900, 1994.

[4] N. Bloembergen. Surface nonlinear optics: a historical overview. *Appl. Phys. B-Lasers O.*, 68(3):289–293, 1999.

[5] J. F. McGilp. Second-harmonic generation at semiconductor and metal surfaces. *Surf. Rev. Lett.*, 6(03n04):529–558, 1999.

[6] G. Lüpke. Characterization of semiconductor interfaces by second-harmonic generation. *Surf. Sci. Rep.*, 35(3):75–161, 1999.

[7] M. C. Downer, Y. Jiang, D. Lim, L. Mantese, P. T. Wilson, B. S. Mendoza, and V.I. Gavrilenko. Optical second harmonic spectroscopy of silicon surfaces, interfaces and nanocrystals. *Phys. Status Solidi A*, 188(4):1371–1381, 2001.

[8] M. C. Downer, B. S. Mendoza, and V. I. Gavrilenko. Optical second harmonic spectroscopy of semiconductor surfaces: advances in microscopic understanding. *Surf. Interface Anal.*, 31(10):966–986, 2001. I

[9] L. Reining, R. Del Sole, M. Cini, and J. G. Ping. Microscopic calculation of second-harmonic generation at semiconductor surfaces: As/Si(111) as a test case. *Phys. Rev. B*, 50(12):8411–8422, 1994. I

[10] S. M. Anderson, N. Tancogne-Dejean, B. S. Mendoza, and V. Véniard. Theory of surface second-harmonic generation for semiconductors including effects of nonlocal operators. *Phys. Rev. B*, 91(7):075302, February 2015. I

[11] J. E. Mejía, B. S. Mendoza, and C. Salazar. Layer-by-layer analysis of second harmonic generation at a simple surface. *Revista Mexicana de Física*, 50(2):134–139, 2004. I

[12] Robert W. Boyd. *Nonlinear Optics*. AP, New York, 2007. II

[13] V. Mizrahi and J. E. Sipe. Phenomenological treatment of surface second-harmonic generation. *J. Opt. Soc. Am. B*, 5(3):660–667, 1988. II, II, II

[14] J. E. Sipe. New Green-function formalism for surface optics. *Journal of the Optical Society of America B*, 4(4):481–489, 1987. II

[15] J. E. Sipe, D. J. Moss, and H. M. van Driel. Phenomenological theory of optical second- and third-harmonic generation from cubic centrosymmetric crystals. *Phys. Rev. B*, 35(3):1129–1141, January 1987. III, II, III A

[16] S. V. Popov, Y. P. Svirko, and N. I. Zheludev. *Susceptibility tensors for nonlinear optics.* CRC Press, 1995. III